Rapid Communications

Unconventional ferromagnetism in epitaxial (111) $LaNiO_3$

Tomoya Asaba,[1] Ziji Xiang,[1] T. H. Kim,[2] M. S. Rzchowski,[3] C. B. Eom,[2] and Lu Li[1]
[1]*Department of Physics, University of Michigan, Ann Arbor, Michigan 48109, USA*
[2]*Department of Materials Science and Engineering, University of Wisconsin-Madison, Wisconsin 53707, USA*
[3]*Department of Physics, University of Wisconsin-Madison, Wisconsin 53706, USA*

(Received 3 December 2017; published 12 September 2018)

We report the observation of ferromagnetism in thin films of paramagnetic metal $LaNiO_3$ grown on nonmagnetic insulating substrate $LaAlO_3$(111) substrates. The films exhibit a large hysteresis loop on magnetoresistance and anomalous Hall effect as well as sixfold anisotropic magnetoresistance. Together with the ferroelectricity and inversion symmetry breaking reported in the same system, these results suggest that, by the geometric constraints by the substrate, paramagnetic metals can turn into ferromagnetic semiconductors. The ferromagnetic ground state is consistent with the predicted spin-split Fermi surfaces of spin-orbit-coupled correlated metals. Moreover, our results reveal a positive linear magnetoresistance and a sign reversal of hysteresis loop, which is consistent with the existence of a massive Dirac point as predicted by theories.

DOI: 10.1103/PhysRevB.98.121105

Transition metal oxides (TMOs) have been intensively studied to understand various quantum phenomena of strongly correlated materials, such as metal-insulator transition, multiferroicity, and high-temperature superconductivity [1,2]. The advances in ultrathin film growth with atomic precision further provide a wide control of lattice constant and geometrical confinement. Most of the previous studies on TMO thin films have been focused on systems grown along the (001) direction. Recently, several theoretical studies have shown that the bilayer TMO grown along the (111) direction are promising candidates for realizing strongly correlated topological phases due to the presence of a buckled graphenelike honeycomb lattice [3].

Among TMOs, in particular, lanthanum nickelate [$LaNiO_3$ (LNO)] has been theoretically studied intensively. $LaNiO_3$ belongs to rare-earth nickelate family $RNiO_3$ (RNO), but LNO is the only metallic compound at all temperatures with nonmagnetic ground state among $RNiO_3$ [4]. Many $LaNiO_3/LaAlO_3$ (LNO/LAO) heterostructures are grown along the (001) direction after the prediction of high-T_c cupratelike physics in this system [5,6]. For (111) direction growth, recent theoretical calculations predict the possibility of topologically nontrivial interacting ground states such as quantum anomalous Hall effect and Dirac half semimetal, as well as multiferroicity (ferroelectricity and ferromagnetism) and metal-insulator transition [7–11]. Despite the intriguing theoretical predictions, however, experimental studies on (111)-oriented RNO thin films have not been very successful due to the difficulty of growth along the strongly polarized (111) interface [12]. The first report on a LNO/LAO superlattice shows insulating behavior rather than the expected Dirac semimetals [13]. More recently, LNO thin films grown on (111) LAO substrate have shown the polar metallic feature indicating ferroelectricity [14]. However, so far no experimental sign of topological features has been reported in the LNO system. Furthermore, while many theoretical calculations predict that the ferromagnetic phase is favored in LNO/LAO thin films [9,11] (and even LSDA + U calculations predict bulk LNO ferromagnetism [15]), no ferromagnetic phase has been observed from LNO heterostructures except for a ferromagnetic $LaMnO_3$ [16] or $CaMnO_3$ [17] superlattice.

In this Rapid Communication, we report the observation of ferromagnetism from $LaNiO_3$ thin films grown on nonmagnetic $LaAlO_3$(111) substrates. With the existence of a ferroelectric metal state reported before [14], LNO/LAO thin films exhibit multiferroicity, shedding light on the application of multiferroic metals. Moreover, positive linear magnetoresistance and the sign reversal of hysteresis loop have been observed. These features are consistent with the presence of a Dirac point. The anisotropic magnetoresistance and planar Hall effect measurement further confirm the preserved C_3 symmetry, which is consistent with the theoretical prediction of a ferromagnetic massive Dirac state.

Epitaxial LNO thin films were synthesized on LAO(111) and (001) substrates by the pulsed laser deposition (PLD) method where the film thickness can be *in situ* monitored during the PLD growth by a RHEED (reflection high-energy electron diffraction) technique. The thickness of the as-grown LNO thin films are about 2.23 and 3.86 nm for the (111) and (001) samples, respectively. Since the unit-layer thickness is 0.223 and 0.386 nm in the pseudocubic (111) and (001) orientations, respectively, both LNO/LAO(111) and (001) thin films are ten layers thick. More details of the sample fabrication can be found in the previous literature [14].

Figure 1 summarizes the angular and temperature dependence of magnetoresistance (MR) for the LNO/LAO(111) thin film. We have measured two samples and the similar behavior was observed. Figure 1(a) shows an angular dependence of MR measured at $T = 3$ K. A clear butterflylike hysteresis loop was observed at each angle. This is evidence of ferromagnetism in LNO/LAO(111). Focusing on the sign of the loop, at around 0° MR is larger when sweeping the magnetic field from zero, indicating that the resistivity is enhanced in

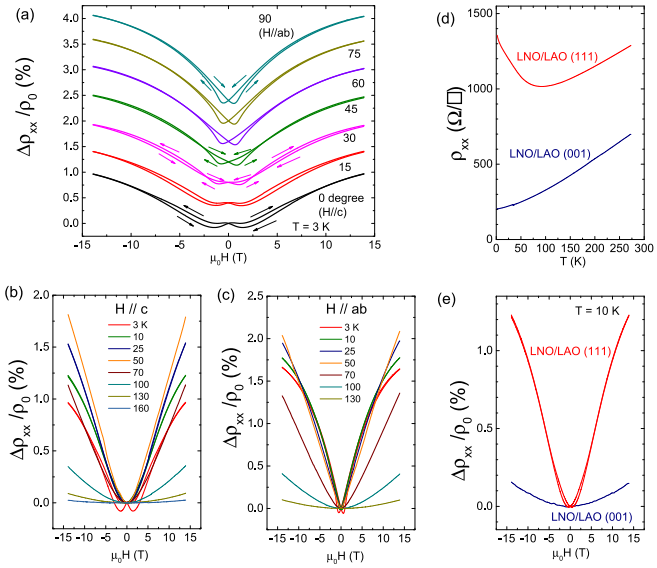

FIG. 1. Angular and temperature dependence of magnetoresistance from $LaNiO_3/LaAlO_3$ thin film. (a) Angular dependence of normalized magnetoresistance $\Delta\rho_{xx}/\rho_0$ at $T = 3$ K between 0 ($H \parallel c$) and 90° ($H \parallel ab$). The curves are vertically displaced by 0.4% for clarity. The arrows mark the direction of the increase of magnetic fields. The current is applied along the $[1\bar{1}0]$ direction, and the magnetic field H is applied always perpendicular to the current. (b),(c) Temperature dependence of $\Delta\rho_{xx}/\rho_0$ at out-of-plane (b) and in-plane (c) field orientations ranging from 3 to 130 K. (d),(e) Temperature (d) and out-of-plane magnetic field (e) dependence of ρ_{xx} for both LNO/LAO(111) and (001) configurations.

the vicinity of the magnetization reversal. This is typical for most of the ferromagnets, as carriers are usually scattered by domain walls. However, at 30°, there is a sign reversal of the hysteresis loop at low fields, whereas at high fields, the domain wall contribution is still positive. Above 30° the conductivity is totally enhanced by the domain wall. Similar behavior has been observed in ferromagnetic topological insulators [18] and topological Kondo insulators [19], and is attributed to chiral conducting modes mediated by the Dirac point.

The weird behavior of MR can be also observed in the temperature dependence, as shown in Figs. 1(b) ($H \parallel c$) and 1(c) ($H \parallel ab$). In both orientations, while between 3 and 10 K the MR shows positive and sublinear behavior at high fields, the MR becomes almost linear between 25 and 50 K. Particularly, in $H \parallel ab$ configuration, the linear behavior continues down to zero field, whereas in $H \parallel c$ configuration MR becomes rounded at zero field. The angular dependence of linearity in a ferromagnet is usually related to anisotropic magnetoresistance (AMR). When the magnetic field is applied parallel to the hard axis, MR is rounded near zero field due to slow magnetization saturation [20]. When the field is applied along the easy axis, the AMR effect decreases and the magnon suppression mechanism becomes dominant, resulting in linear MR. Thus, the ab plane is expected to be an easy axis (easy plane). However, in ferromagnetic materials, magnon suppression usually makes MR negatively linear, not positively linear.

Recently, it has been reported that ferromagnetic topological insulator $Cr_{0.15}(Bi_{0.1}Sb_{0.9})_{1.85}Te_3$ shows positive linear MR when the gate voltage is tuned so that the Fermi level lies near the Dirac point, while MR becomes negative when the Fermi level lies way below or above the Dirac point [21]. The strong connection between the Dirac point and positive linear MR in time-reversal-symmetry-broken materials is also indicated in one of the Dirac material candidates $Bi_2Ir_2O_7$ [22], which shows both hysteresis loop and positive linear MR.

We note the difference between $LaNiO_3$ thin films grown on $LaAlO_3(111)$ substrate and $LaAlO_3(001)$ substrate. The temperature dependence of resistance for both configurations is shown in Fig. 1(d). LNO(001) thin film not only shows much smaller resistivity than LNO(111) thin films, it also shows the metallic temperature dependence down to $T = 20$ mK. This is consistent with the previous reports [23] and also similar to the bulk $LaNiO_3$, a paramagnetic metal. On the other hand, LNO/LAO(111) shows metal-insulator transition (MIT) at around 100 K. This kind of MIT has been observed in other $RNiO_3$ families, and indeed $LaNiO_3$ is the only metallic compound. Especially, in $NdNiO_3$ (NNO) thin film, MIT can be controlled by the lattice mismatch between NNO and the substrate, and resistivity versus temperature curve shows a small upturn on the boundary of metal and insulator phase [24]. We also note that the gapped behavior at low T is consistent with the predicted gapped Dirac semimetal. The MR behavior is also quite different between LNO/LAO(111) and LNO/LAO(001). In LNO/LAO(001), MR is one order of magnitude smaller than that from LNO/LAO(111) shown in Fig. 1(e), and shows no linear behavior. This behavior is almost the same as bulk and thin film studies grown on $LaAlO_3$ substrates reported previously [23], while negative MR was reported in $LaAlO_3$ thin films grown on $SrTiO_3$ substrates [25–27].

Another strong evidence of ferromagnetism is anomalous Hall effect (AHE). In a ferromagnetic material, ρ_{yx} is expressed as

$$\rho_{xy} = R_H B + \mu_0 R_s M, \tag{1}$$

where R_H and R_s are ordinary and anomalous Hall coefficients. We display the angular dependence of the AHE at $T = 3$ K in Fig. 2(a). Clear large hysteresis loops are observed when the magnetic field is applied parallel to the c axis, while the anomalous Hall coefficient is quickly saturated at low fields when the magnetic field gets close to the plane. This is consistent with the easy-plane picture. Furthermore, the nonzero ρ_{xy} at zero fields suggests the spontaneous magnetization, confirming the existence of magnetic ordering. Also, the hysteresis loop persists up to 13 T. Such a strong coercive field also indicates ferromagnetic ordering.

The temperature dependence of the AHE is shown in Fig. 2(b). At $T = 25$ K, the hysteresis loop becomes very small and at $T = 50$ K no anomalous Hall component was observed, indicating that T_c is around 50 K. Above 50 K, ρ_{yx} is almost linear and the calculated carrier density is similar to that from the bulk $LaNiO_3$ or thin $LaNiO_3$ film grown on (001) $LaAlO_3$ [Fig. 2(c)]. This fact indicates that the doping effect by the lattice strain is relatively small, but rather the magnetism is affected by the symmetry of thin

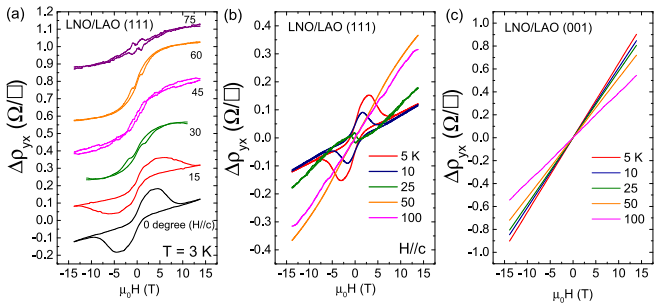

FIG. 2. Anomalous Hall effect from $LaNiO_3/LaAlO_3(111)$ and (001) thin films. (a) Angular dependence of AHE with applied magnetic field tilted from 0 to 75°, taken at $T = 3$ K. Curves are displaced by 0.2 Ω/square for clarity. (b) Hysteresis loops of ρ_{yx} at selected T. The magnetic field is applied perpendicular to the film plane. (c) ρ_{yx} at selected T from LNO/LAO(001).

films, e.g., strain orientation. From the hysteresis loop and AHE, it is inferred that the system is ferromagnetic. This is further supported by nonzero ρ_{xy} at zero fields, indicating the spontaneous magnetization in the sample.

The symmetry of the system could be reduced from undistorted P_{321} to P_3 or even fully distorted P_1 due to the strain, and it is predicted that the symmetry plays a key role on whether the system is Dirac material or multiferroic [11]. When the lattice is undistorted and in P_{321} symmetry, the system is predicted to be ferromagnetic Dirac half-semimetal. With broken inversion symmetry due to the lattice strain, the symmetry is reduced to P_3 and the system becomes multiferroic (ferroelectric and ferromagnetic) with the Dirac point gapped (massive Dirac). When the lattice symmetry is fully broken and becomes P1, the system is still multiferroic and gapped, but the Dirac point no longer exists. Thus, it is important to check if the symmetry of the system (especially C_3) is broken or not.

To solve this issue, we have measured in-plane AMR and planar Hall effect (PHE). In polycrystals, the angular dependence of AMR and PHE depends on the angle between the current and magnetic field, and is dominated by twofold components. However, in a crystalline system, AMR only depends on θ and ϕ, where θ (ϕ) is the angle between magnetic field (current) and a certain crystal axis ([1$\bar{1}$0] for our case). The angular dependence of AMR $\Delta\rho_{xx}(\theta, \phi)$ reflects the crystal symmetry. For a hexagonal system [28], $\Delta\rho_{xx}(\theta, \phi)$ is given by

$$\Delta\rho_{xx}(\theta, \phi) = C_2 \cos(2\theta - 2\phi) + C_4 \cos(4\theta + 2\phi) + C_6 \cos(6\theta), \quad (2)$$

where C_2, C_4, and C_6 are AMR coefficients for two-, four-, and sixfold components. Similarly, the angular dependence of PHE in a hexagonal system is given by

$$\Delta\rho_{yx}(\theta, \phi) = C_2 \sin(2\theta - 2\phi) - C_4 \sin(4\theta + 2\phi). \quad (3)$$

Note that the sixfold component vanishes in PHE. This is quite different from the square lattice case, where C_6 exists instead of the vanishing C_4 component in the PHE effect. Thus, the absence of C_6 and the existence of C_4 confirm that the magnetic structure is hexagonal.

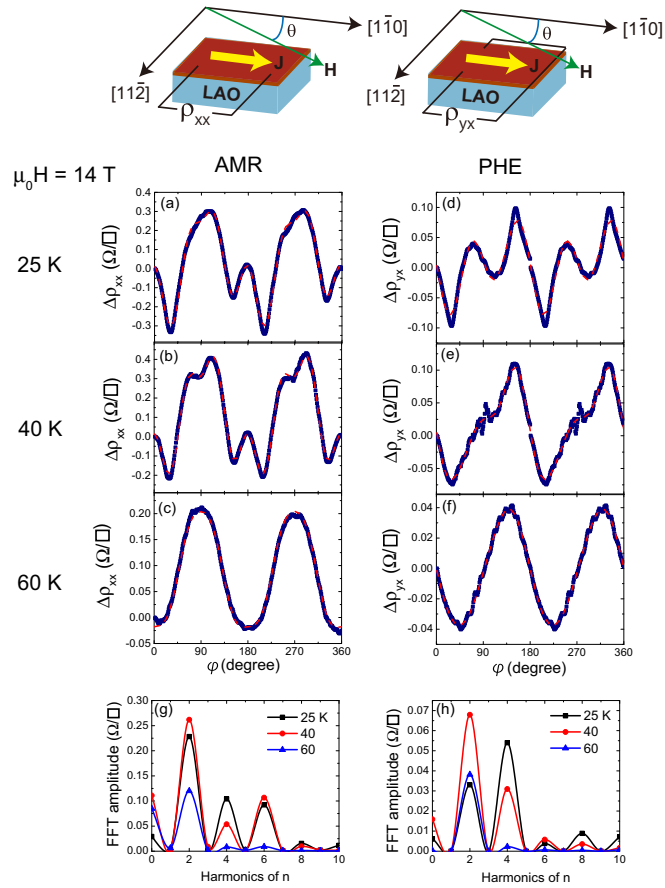

FIG. 3. Anisotropic magnetoresistance and planar Hall effect at selected T. (a)–(c) Angular dependence of anisotropic magnetoresistance at $T = 25$, 40, and 60 K, respectively. The current is applied to the [1$\bar{1}$0] direction. Magnetic field is applied in-plane with angle θ from the [1$\bar{1}$0] axis. Red dashed lines are fitting curves using Eq. (2). Fitting parameter of ϕ is around 4°, indicating the misalignment between the current and the [1$\bar{1}$0] axis. (d)–(f) Angular dependence of planar Hall effect with the same condition as AMR. Red dashed lines are fitting curves using Eq. (3). Due to small out-of-plane misalignment ($\sim 1°$), the signal was symmetrized to eliminate the contribution from ordinary and anomalous Hall effect. (g),(h) Fast Fourier transformation (FFT) plot of the data in (a)–(f) displays as a function of harmonic numbers.

The angular dependence of ρ_{xx} and ρ_{yx} with $H = 14$ T at different temperatures are shown in Figs. 3(a)–3(f). At temperatures lower than $T = 25$ K, the angle sweep-up and sweep-down show different behavior, indicating that the magnetization is not fully polarized. At higher T, both AMR and PHE are fit well by Eqs. (2) and (3). Particularly, below $T = 50$ K the sixfold (fourfold) component was clearly observed in AMR (PHE), while above $T = 60$ K the signal is dominated by the twofold component, indicating that the critical temperature is around $T = 60$ K, consistent with AHE measurements. This is more clearly seen in fast Fourier transform (FFT) plots [Figs. 3(g) and 3(h)]. Furthermore, the sixfold component shown in AMR but not in PHE indicates the presence of C_3 symmetry. This is consistent with P_{321} or P_3 symmetry, with which the theory predicts the existence of a Dirac point [11]. However, it contradicts with the monoclinic symmetry with

three equivalent domains determined by the optical second-harmonic generation measurement [14]. Another possibility is that the angular dependence of AMR and PHE results from a magnetic domain distribution. Since the typical magnetic domain size is of the order of 100 nm or larger, it is possible that the structural domain information is smeared out by the magnetic domain.

The robust hysteresis loop, the existence of AHE, and the AMR and PHE suggest the magnetic ordering, especially a ferromagnetic ground state, in the films of LNO/LAO(111). Although the hysteresis loop and AHE have also been observed in antiferromagnetic systems with canted magnetic moments, the large coercive field ($\sim$13 T) points most likely to a ferrmomagnetic ground state. The positive linear MR observed in $H \parallel ab$ orientation is striking, since it excludes most of the possibilities related to quantum interference. It is known that the two-dimensional disorder-induced quantum interference has a $\ln B$ dependence of magnetic field. Thus, the combination of $\ln B$ and parabolic MR from classical orbital effect could result in the linear behavior of MR. However, since the magnetic field is applied in-plane, the classical MR contribution cannot be large. Also, weak localization and weak antilocalization can be ruled out, as they are considered to be orbital effect and highly affected by a perpendicular component of H. Nevertheless, the in-plane MR is even larger than that from out-of-plane in our case. Furthermore, given that LNO/LAO(001) shows one order of magnitude smaller MR with no linear behavior, it is hard to think that the disorder effect is dominant in LNO/LAO(111). Thus, we can rule out this possibility. Linear positive MR has been also reported in thin ferromagnetic films [29]. In this case, linear MR originates from disorder, and it should be isotropic. Again, this contradicts with our angular dependence of MR. Therefore this possibility can be ruled out as well, and we conclude that the positive linear MR comes from the intrinsic effect. From the theoretical prediction, the LNO/LAO(111) system with P_3 symmetry becomes multiferroic with the gapped Dirac point. All our observations are consistent with this picture: sign reversal of hysteresis loop, positive linear MR, ferromagnetic and ferroelectric features, the gapped behavior of temperature dependence of resistivity at low T, and C_3 symmetry observed in in-plane AMR. Surprisingly, however, in $NdNiO_3/LaAlO_3$(111) and $LaNiO_3/LaAlO_3$(111) thin films, the rotational symmetry as well as inversion symmetry are found to be broken [14]. There are a few explanations. First, it is possible that the AMR and PHE could not tell the difference between P_3 and P_c (monoclinic) with three equivalent domain variants with the angle of 120° between each domain. Since the origin of AMR is the spin-dependent scattering of conducting electrons led by spin-orbit coupling, its length scale could be longer than the domain size. In this case, the theory predicts that the system is still multiferroic, but the Dirac point no longer exists. Also, it is possible that the system is partially detwinned by the magnetic field, similar to that observed in iron-based superconductors [30,31]. If this is the case, the calculation predicts that gap opening happens at the K point.

Finally, it is worth pointing out the electron-driven parity-breaking phase as a possible origin of multiferroicity in LNO/LAO(111). A similar ferroelectric metal phase has been reported in the bulk $LiOsO_3$ [32], accompanied by the structural transition at 140 K where the inversion symmetry disappears. This effect is argued to originate from the inversion symmetry breaking induced by the electron correlation in spin-orbit-coupled correlated metals [33]. In the theory, the p-wave spin-spin interaction leads to spin-split Fermi surfaces and gives rise to a polarization of electrons. Similarly, in LNO/LAO(111), despite the C_3 symmetry of LAO substrate, the inversion symmetry is broken up to room temperature, which leads to ferroelectricity [14]. The transition is accompanied by the Fermi surface spin splitting, which lays the foundation for the magnetic ordering.

In summary, we first observed the magnetically ordered state of $LaNiO_3$ thin film grown on $LaAlO_3$(111) substrate as predicted by many groups. This result is important not only because it gives further guidance to improve the theoretical calculation, but also, with the ferroelectric feature reported before, it sheds light on the application to the spintronics. Moreover, our results are consistent with the existence of a gapped Dirac point predicted by the theory. These results would be a significant step forward in the realization of a strongly correlated topological phase by geometrical engineering of a buckled honeycomb lattice.

This work is supported by the Office of Naval Research through the Young Investigator Prize under Award No. N00014-15-1-2382 (electrical transport characterization), by the National Science Foundation under Award No. DMR-1707620 (test of magnetization measurements), by the US Department of Energy (DOE), Office of Science, Office of Basic Energy Sciences (BES), under Award No. DE-FG02-06ER46327 (thin film growth and structural characterizations), and the National Science Foundation Major Research Instrumentation award under Award No. DMR-1428226 (supports the equipment for the electrical transport characterizations).

[1] M. Imada, A. Fujimori, and Y. Tokura, Rev. Mod. Phys. **70**, 1039 (1998).

[2] N. P. Armitage, P. Fournier, and R. L. Greene, Rev. Mod. Phys. **82**, 2421 (2010).

[3] D. Xiao, W. Zhu, Y. Ran, N. Nagaosa, and S. Okamoto, Nat. Commun. **2**, 596 (2011).

[4] J. B. Torrance, P. Lacorre, A. I. Nazzal, E. J. Ansaldo, and C. Niedermayer, Phys. Rev. B **45**, 8209 (1992).

[5] J. Chaloupka and G. Khaliullin, Phys. Rev. Lett. **100**, 016404 (2008).

[6] P. King, H. Wei, Y. Nie, M. Uchida, C. Adamo, S. Zhu, X. He, I. Božović, D. Schlom, and K. Shen, Nat. Nanotechnol. **9**, 443 (2014).

[7] K.-Y. Yang, W. Zhu, D. Xiao, S. Okamoto, Z. Wang, and Y. Ran, Phys. Rev. B **84**, 201104 (2011).

[8] A. Rüegg and G. A. Fiete, Phys. Rev. B **84**, 201103 (2011).

[9] A. Rüegg, C. Mitra, A. A. Demkov, and G. A. Fiete, Phys. Rev. B **85**, 245131 (2012).
[10] A. Rüegg, C. Mitra, A. A. Demkov, and G. A. Fiete, Phys. Rev. B **88**, 115146 (2013).
[11] D. Doennig, W. E. Pickett, and R. Pentcheva, Phys. Rev. B **89**, 121110 (2014).
[12] J. Blok, X. Wan, G. Koster, D. H. Blank, and G. Rijnders, Appl. Phys. Lett. **99**, 151917 (2011).
[13] S. Middey, D. Meyers, M. Kareev, E. Moon, B. Gray, X. Liu, J. Freeland, and J. Chakhalian, Appl. Phys. Lett. **101**, 261602 (2012).
[14] T. Kim, D. Puggioni, Y. Yuan, L. Xie, H. Zhou, N. Campbell, P. Ryan, Y. Choi, J.-W. Kim, J. Patzner *et al.*, Nature (London) **533**, 68 (2016).
[15] G. Gou, I. Grinberg, A. M. Rappe, and J. M. Rondinelli, Phys. Rev. B **84**, 144101 (2011).
[16] M. Gibert, P. Zubko, R. Scherwitzl, J. Íñiguez, and J.-M. Triscone, Nat. Mater. **11**, 195 (2012).
[17] A. J. Grutter, H. Yang, B. J. Kirby, M. Fitzsimmons, J. A. Aguiar, N. D. Browning, C. Jenkins, E. Arenholz, V. Mehta, U. Alaan *et al.*, Phys. Rev. Lett. **111**, 087202 (2013).
[18] J. G. Checkelsky, J. Ye, Y. Onose, Y. Iwasa, and Y. Tokura, Nat. Phys. **8**, 729 (2012).
[19] Y. Nakajima, P. Syers, X. Wang, R. Wang, and J. Paglione, Nat. Phys. **12**, 213 (2016).
[20] J. G. Checkelsky, M. Lee, E. Morosan, R. J. Cava, and N. P. Ong, Phys. Rev. B **77**, 014433 (2008).
[21] Z. Zhang, X. Feng, M. Guo, K. Li, J. Zhang, Y. Ou, Y. Feng, L. Wang, X. Chen, K. He *et al.*, Nat. Commun. **5**, 4915 (2014).
[22] J.-H. Chu, S. C. Riggs, M. Shapiro, J. Liu, C. R. Serero, D. Yi, M. Melissa, S. Suresha, C. Frontera, A. Vishwanath, X. Marti, I. Fisher, and R. Ramesh, arXiv:1309.4750.
[23] J. Son, P. Moetakef, J. M. LeBeau, D. Ouellette, L. Balents, S. J. Allen, and S. Stemmer, Appl. Phys. Lett. **96**, 062114 (2010).
[24] J. Liu, M. Kargarian, M. Kareev, B. Gray, P. J. Ryan, A. Cruz, N. Tahir, Y.-D. Chuang, J. Guo, J. M. Rondinelli *et al.*, Nat. Commun. **4**, 2714 (2013).
[25] R. Scherwitzl, S. Gariglio, M. Gabay, P. Zubko, M. Gibert, and J.-M. Triscone, Phys. Rev. Lett. **106**, 246403 (2011).
[26] J. Zhang, W.-J. Ji, J. Xu, X.-Y. Geng, J. Zhou, Z.-B. Gu, S.-H. Yao, and S.-T. Zhang, Sci. Adv. **3**, e1701473 (2017).
[27] R. Mallik, E. Sampathkumaran, and P. Paulose, Appl. Phys. Lett. **71**, 2385 (1997).
[28] P. K. Rout, I. Agireen, E. Maniv, M. Goldstein, and Y. Dagan, Phys. Rev. B **95**, 241107 (2017).
[29] A. Gerber, I. Kishon, I. Y. Korenblit, O. Riss, A. Segal, M. Karpovski, and B. Raquet, Phys. Rev. Lett. **99**, 027201 (2007).
[30] J.-H. Chu, J. G. Analytis, D. Press, K. De Greve, T. D. Ladd, Y. Yamamoto, and I. R. Fisher, Phys. Rev. B **81**, 214502 (2010).
[31] Y. Xiao, Y. Su, S. Nandi, S. Price, B. Schmitz, C. M. N. Kumar, R. Mittal, T. Chatterji, N. Kumar, S. K. Dhar, A. Thamizhavel, and T. Brückel, Phys. Rev. B **85**, 094504 (2012).
[32] Y. Shi, Y. Guo, X. Wang, A. J. Princep, D. Khalyavin, P. Manuel, Y. Michiue, A. Sato, K. Tsuda, S. Yu, M. Arai, Y. Shirako, M. Akaogi, N. Wang, K. Yamaura, and A. T. Boothroyd, Nat. Mater. **12**, 1024 (2013).
[33] L. Fu, Phys. Rev. Lett. **115**, 026401 (2015).